International Journal of Environmental Sciences
ISSN: 2229-7359
Vol. 11 No. 5, 2025
https://theaspd.com/index.php

Comparative Synthesis of N-TiO_2 Photocatalysts via Green and Chemical Routes for Enhanced Photocatalytic Performance

[a]**Dilan Nawzad Mamakhan,** [b]**Nabil Adil Fakhre**
[a]Chemistry Department, Education College, Salahaddin University-Erbil, Iraq, dilan.mamakhan@su.edu.krd,
[b] Tishk International University, nabil.fakhre@su.edu.krd

Abstract
To improve the visible light-driven photocatalytic activity of TiO_2, nitrogen-doped (N-TiO_2) nanoparticles were prepared through two different methods: a green method using Taraxacum officinale flower extract and a traditional chemical precipitation method. The structural, morphological, elemental, and optical properties of the resultant N-TiO_2 samples were comprehensively examined by X-ray diffraction, Fourier-transform infrared spectroscopy, UV–Vis diffuse reflectance spectroscopy, Scanning and Transmission electron microscopy, and energy-dispersive X-ray spectroscopy (EDS). Both preparation methods resulted in anatase-phase TiO_2 with successful nitrogen doping; however, the green-synthesized N-TiO_2 displayed a smaller average crystallite size (~30 nm), greater nitrogen content (3.83 wt.%), and narrower band gap of 2.8 eV compared to its chemically synthesized counterpart. Photocatalytic activity was assessed through the degradation of methyl orange under visible light illumination. The green-synthesized N-TiO_2 attained a degradation efficiency of 86.6% within 120 minutes, outperforming the chemically synthesized sample (73.3%). The superior activity is ascribed to enhanced charge carrier separation and synergistic effects of bio-compound surface functionalities. This study illustrates the efficacy of green synthesis in the production of environmentally friendly and highly active N-TiO_2 photocatalysts, showing great potential for wastewater treatment and organic pollutant degradation under visible light.
keyword: *Green synthesis, Chemical synthesis, N-TiO_2, photocatalytic degradation*

Graphical abstract

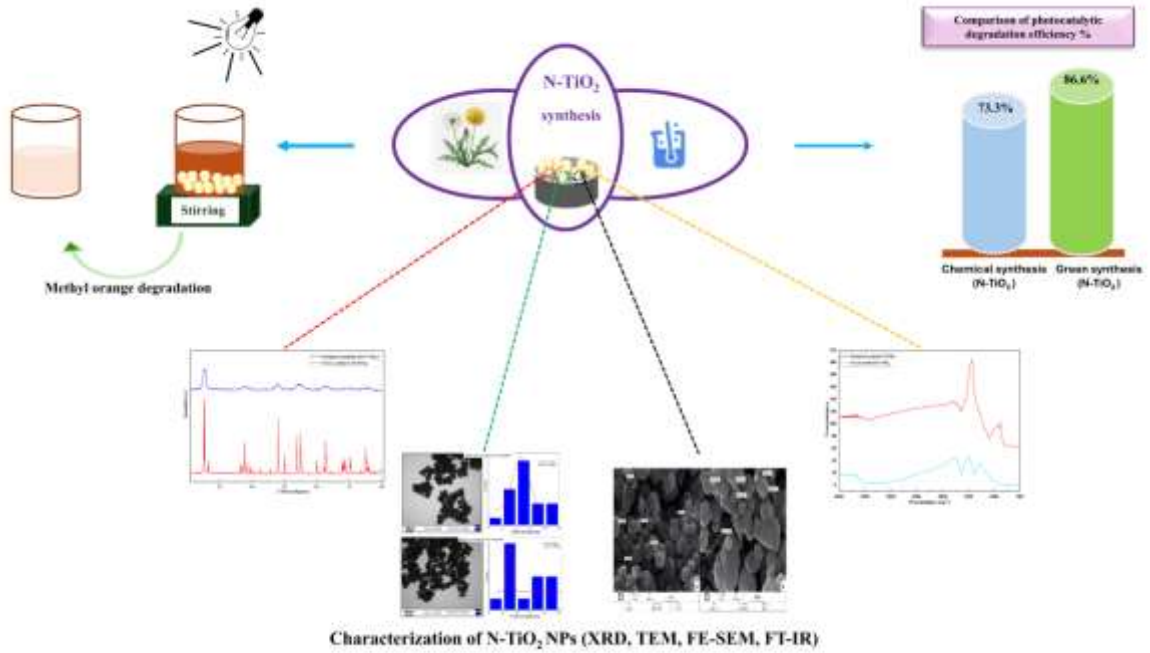

INTRODUCTION

Nanomaterials, defined as substances with dimensions below 100 nm, exhibit distinctive chemical, physical, electrical, and mechanical properties. They are widely employed in various disciplines such as medicine, biotechnology, microbiology, pharmaceuticals, chemistry, engineering, economic catalysis, and cytotoxicity investigation, among others[1]. Due to its extensive surface area, nanomaterial synthesis techniques are categorized into physical and chemical processes[2]. Over the last several decades, metal oxide semiconductors, including ZnO, MgO, CuO, CdO, and NiO, have been extensively used and are synthesized using physical, chemical, and biological techniques[3-4]. TiO_2 nanoparticles are recognized as semiconductors with a broad bandgap of 3.2 eV for the anatase phase and 3.0 eV for the rutile phase, whereas the brookite phase is seldom synthesized[5]. The anatase and rutile phases of TiO_2 possess a tetragonal crystal structure, while the brookite phase has an orthorhombic structure[6]. Titanium dioxide (TiO2), a transition metal oxide, is extensively used in cosmetics, photocatalysts[7], pharmaceuticals[8], sensors[9], and solar cells [10] applications due to its unique characteristics, including interconnected pores and a substantial surface area. Nonetheless, its inherent high band gap (about 3.2 eV for the anatase crystalline phase) considerably limits its effective use of the visible segment of the solar spectrum, which constitutes the majority of incoming solar light [11]. Certain doping tactics have been used to alleviate this constraint and broaden the photo response into the visible spectrum. Multiple studies examined the enhancement of TiO_2 efficiency under visible light by the doping of non-metal and metal elements, namely carbon, phosphorus, bromine, and nitrogen as non-metal dopants, and silver, copper , and iron as metal dopants [12]. Among them, N-TiO_2 nanoparticles have been particularly significant. The introduction of nitrogen induces discrete electronic states in the band gap, which effectively narrows the band gap energy and promotes charge carrier separation, greatly improving photocatalyst activity under visible-light illumination[13].

Specifically interesting are plant extracts from species such as Chromolaena *odorata* leaf extract[14], mangrove aqueous leaf extract[15], which have been successfully used for green synthesis of N-TiO_2 nanoparticles, leading to photocatalysts that exhibit good photocatalytic and antimicrobial activities. Bio-inspired methods are exceptionally beneficial for producing environmentally friendly photocatalysts for applications. Green synthesis employs bio-derived materials such as natural reducing agents, plant extracts, and bio-wastes as eco-friendly options that trigger the nucleation and stabilization of N-TiO_2 nanoparticles at ambient or near-ambient conditions. The bio-mediated process minimizes the production of toxic byproducts, energy utilization, and aligns with principles of sustainable nanomaterials development[16].

N-TiO2 nanoparticles are synthesized through various physical and chemical methods, including microwave-assisted processing[17], hydrothermal synthesis [18], Plasma-Assisted Electrolysis[19], solid-state reaction [20], sol–gel methods[21], Chemical vapor deposition[22], solvothermal crystallization[23], ultrasonic irradiation[12], and green synthesis processes. While effective, most of these conventional processes have high energy consumption and toxic chemicals, such as reducing, stabilizing agents, and artificial capping that tend to form environmentally toxic by-products.

To address this significant knowledge gap, the present research study rationally compares the physicochemical, optical, and photocatalytic performance characteristics of N-TiO_2 nanoparticles synthesized via green bio-compound and conventional chemical precipitation routes. The comprehensive characterization is aimed at understanding the influence of synthesis route on dopant incorporation efficiency, defect chemistry, and overall catalytic activity with a perspective to contributing significantly towards the design of environmentally benign high-performance photocatalysts. These kinds of developments are of significant importance to a broad array of environmental cleanup processes, from water purification to pollutant degradation and heavy metal detoxification.

Fig 1: Green synthesis of N-TiO_2 NPs

Fig 2: Green synthesis of N-TiO_2 NPs

Materials

All reagents were of analytical quality and used without further purification. Titanium tetra isopropoxide (TTIP C12H28O4Ti, 97%) was obtained from Sigma-Aldrich. Urea (H2NCONH2, 98.0%), hydrochloric acid (37% w/w), ammonia (25% w/w), hydrogen peroxide (35%), and acetonitrile were procured from Merck, Germany.

2.1 Preparation of Dandelion Flower Extract

The dandelion flowers (Taraxacum officinale, Asterales) were collected from the Kurdistan area of Iraq. The flower was cleansed with deionized water to eliminate impurities and then dried. The desiccated substance was meticulously ground into a powder. Ten grams of flower powder were incorporated into a beaker containing 100 milliliters of deionized water (DI) to prepare the plant extract. The solution was thereafter heated to 80 °C on a hot plate while being continuously stirred for one hour. The extract of the yellow flower was filtered and cooled to room temperature. The cooled floral extract is used to synthesize nitrogen-TiO_2.

2.2 Green Synthesis of N-TiO_2 NPs

Nitrogen-TiO_2 were synthesized via a green process, as shown in **Fig 1**, with the use of Taraxacum officinale (dandelion) flower extract as a green reducing and capping agent. In the normal process, 5.0 mL of (TTIP) was stirred with 20.0 mL of ethanol for 30 minutes, and then gradually added the dandelion extract. Separately, 2.0 g of urea was dissolved in 50.0 milliliters of DI and slowly added as a dopant for nitrogen. The solution was refluxed at 100°C for 5 hrs. The pH level was adjusted to 9.0 with 1.0 M ammonia solution, and the suspension was aged for 12 hours. The as-prepared (N-TiO_2) NPs were collected by centrifugation at 8000 rpm for 15 minutes and precipitated in a pale-yellow color. The product was washed with DI and ethanol, dried at 80 °C, and calcined at 300 °C for 3 hrs.

2.3 Chemical Synthesis of N-TiO_2 NPs

The N-TiO_2 was prepared through a chemical synthesis route, as shown in Figure 1. To 50.0 milliliter of absolute ethanol under magnetic stirring, 10.0 mL of titanium (IV) isopropoxide (TTIP) was added and maintained for 30 minutes for complete mixing. Meanwhile, 2.0 g of urea was dissolved in 50 mL of DI as the nitrogen precursor. The solution of urea was then dropwise added to the solution of TTIP-ethanol under stirring to enable homogeneous dispersion and control of hydrolysis. The resulting solution was refluxed for 5.0 hours at 100 °C to allow the nitrogen to species to be adsorbed into the lattice of TiO_2. The pH was subsequently adjusted to 3.0 using 1.0 M hydrochloric acid (HCl) to control the equilibrium of hydrolysis-condensation. After 12 hours of aging, the mixture was recovered by centrifugation at 8000 rpm for 15 minutes. The light-yellow precipitate obtained was thoroughly washed with deionized water and ethanol to remove residual impurities, dried at 100 °C, and finally calcined at 300 °C for 3 hours to induce crystallinity and stabilize the doped structure.

2.4 Material Characterization

Various approaches were used to characterize the produced nanoparticles. A Rigaku D/MAX III X-ray Diffraction system with Cu Kα (λ=0.15406 nm) was used for XRD investigation at 40 kV and 30 mA. EDS, FE-SEM, and TEM were used with the "FE-SEM TESCAN MIRA4" and "ZEISS MODEL EM10C" to examine the object's elemental composition and morphological characteristics. FT-IR was conducted using the Shimadzu Spectrum One (IRTracer-100), while the Shimadzu UV-2600 spectrometer was used to assess the optical properties using UV-Vis-DRS.

2.5 Photocatalytic Activity Measurement

Methyl orange serves as a model contaminant for photodegradation studies. Introduce 60 mg of N-TiO_2 nanoparticles into a 250milliliter beaker containing 100 milliliters of methylene orange (MO) solution and subject the mixture to ultrasonication for 10 minutes. Moreover, the combined solution was maintained in dark conditions to achieve absorption-desorption equilibrium. The solution was irradiated under visible light (300W lamp) in a photoreactor for (15, 30 ,60 ,90 ,120 min), and 5 mL of the liquid was extracted at intervals and subjected to centrifugation, with the concentration being measured on a UV-Visible spectrophotometer (Shimadzu). The discoloration rate of the MO solution is determined using the Equation (1)

$$\boldsymbol{decolorization} = \frac{(C0-C)}{C0} \times 100 = \% \qquad \textbf{Equation (1)}$$

where C0 represents the concentration of MO at adsorption-desorption equilibrium in darkness, and C denotes the concentration of methyl orange after the photocatalytic process is completed under visible light irradiation. This approach eliminates the impact of the adsorption quantity of MO on its discoloration rate in solution.

RESULTS AND DISCUSSION

Comparison of synthesis N-TiO_2 NPs

Nitrogen-TiO_2 nanoparticles were synthesized successfully using both chemical and green approaches, with some merits in dopant insertion and process benignity. In the chemical process, TTIP was used as the titanium precursor, while urea was used as the dopant for nitrogen. Acidic conditions of pH 3.0 adjusted enabled controlled hydrolysis and condensation of TTIP with the production of homogeneous particle formation and increased nitrogen incorporation following calcination at 300 °C[24]. Contrarily, green synthesis employed Taraxacum officinale extract as a natural stabilizing and reducing agent. The process was conducted at room temperature with pH adjusted to 9.0 using ammonia for improved alkaline-mediated nucleation and particle stabilization. pH is a vital parameter in titanium dioxide alkoxide hydrolysis and affects morphologically, crystallite size, and doping yield of TiO_2 nanostructures[25]. The yellowish precipitate in both cases indicated successful nitrogen doping, which was likely due to substitutional or interstitial incorporation of nitrogen atoms into the TiO_2 lattice. While the two methods produced comparable optical properties of doped nanoparticles, the green process offered a sustainable approach by reducing chemical burden and utilizing phytochemicals derived from plants for stabilizing nanoparticles and morphological control.

XRD analysis

X-ray diffraction characterized the crystalline phase, structure, purity, and average crystallite size of Nitrogen-TiO_2 nanoparticles. As can be seen from **Fig *3***, the green and chemically synthesized N-TiO_2 nanoparticles show prominent diffraction peaks at 2θ values of 25.32°, 36.99°, 37.84°, 48.07°, 53.95°, 55.109°, 62.75°, 68.85°, and 70.35°, corresponding to the (110), (101), (111), (210), (211), (220), (002), and (301) Bragg reflection planes, respectively[26]. Confirming that the anatase crystalline phase predominates in the synthesized nanoparticles. The peak intensity at 25.32° (101) indicates the high crystallinity of the N-TiO_2 NPs from green synthesis samples.

$$D = \frac{K\lambda}{\beta COS\theta}$$

The average crystallite size was estimated using the Debye–Scherrer equation with D as the crystallite size, K as the shape factor (0.89), ($\lambda = 1.5406$ Å) as the X-ray wavelength, β as the full width at half maximum (FWHM), and θ as the Bragg angle[27]. The theoretically calculated average crystallite size in the green and chemically synthesized N-TiO_2 NPs samples was 24.7–53.6 nm, in good accordance with available data. Minimal peak intensity, phase, and crystallite size fluctuations were observed in the samples, which were a consequence of the variation in the synthesis protocol. Notably, the green synthesis N-TiO_2 NPs exhibited more intense and sharper peaks, which may be due to the capping and stabilization effect by polyphenolic compounds present in the plant extract.

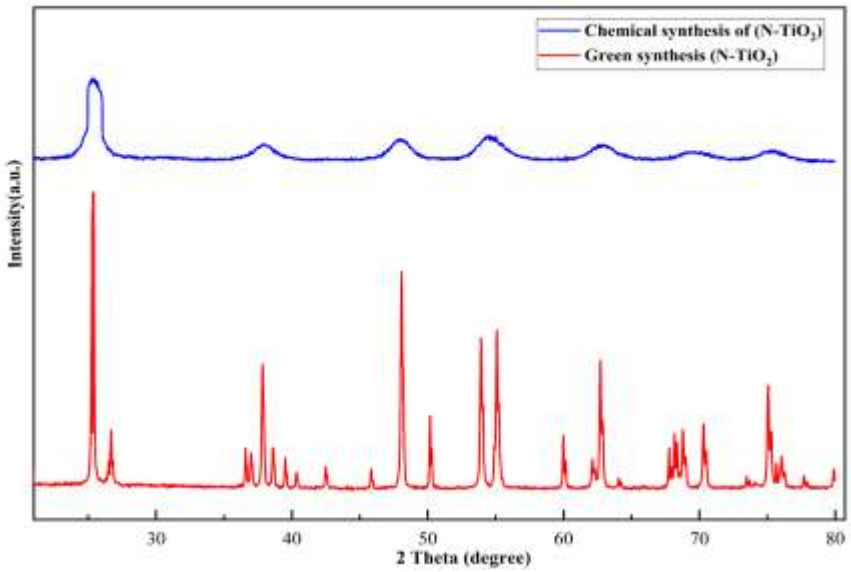

Fig 3: XRD pattern for green and chemical synthesis of N-TiO_2 nanoparticles

FE-SEM with EDS and TEM analysis

The particle morphology and size of the surface of (N-TiO_2) synthesized were characterized using FES-SEM and TEM, as shown in **Fig 4**(a and b). FE-SEM images confirm that green-synthesized N-TiO_2 nanoparticles possess a more dispersed and spherical surface morphology. The chemically synthesized N-TiO_2 samples, however, exhibit somewhat aggregated but still sphere-like surface morphology[28]. This morphological difference can be attributed to variations in the conditions of synthesis and the influence of natural bio compounds present in the green path, acting as stabilizing and capping agents. The estimated average particle size from FE-SEM micrographs ranges between 24-80 nm for green synthesis and 34-122 nm for chemical synthesis. Energy-dispersive X-ray spectroscopy analysis **Fig 4**(c and d), also corroborates the presence of titanium, nitrogen, and oxygen in both samples. Chemically synthesized N-TiO_2 contains a higher oxygen content (76.04 wt.%) and marginally lower nitrogen incorporation (2.57wt.%) relative to the green synthesized sample, which contains (66.25 wt.%) oxygen and (3.83 wt.%) nitrogen. The relatively higher nitrogen content of the green synthesized N-TiO_2 can be ascribed to more effective nitrogen precursor incorporation during synthesis, because of the plant-derived stabilizing agents used, whereas the chemical route possibly hinders nitrogen doping. Nonetheless, both routes confirm successful nitrogen doping of TiO_2.

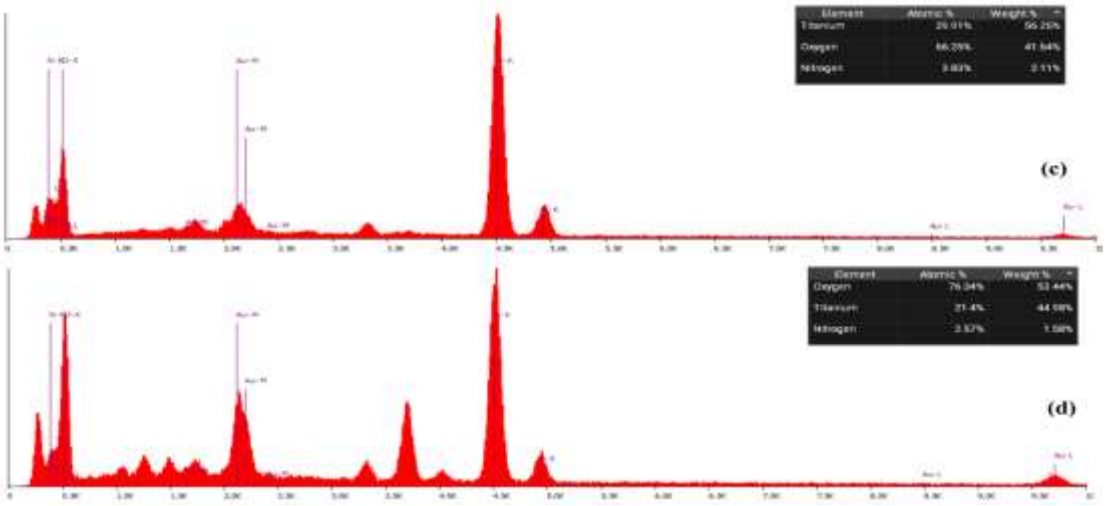

As shown in Fig. 4, the TEM images reveal that both samples consist of approximately spherical particles. However, the green-synthesized N-TiO_2 exhibits better dispersion and smaller particle size compared to the chemically synthesized sample.

For the green-synthesized N-TiO_2 nanoparticles (Fig. 4a), the particles are well-dispersed with minimal agglomeration. The particle size histogram indicates a mean diameter of **30 ± 6 nm**, suggesting a uniform nucleation and growth process facilitated by bioactive compounds in the green precursor. This reduced and more consistent particle size enhances surface area and photocatalytic activity [29].

In contrast, the chemically synthesized N-TiO_2 nanoparticles (Fig. 4b) display a broader particle size

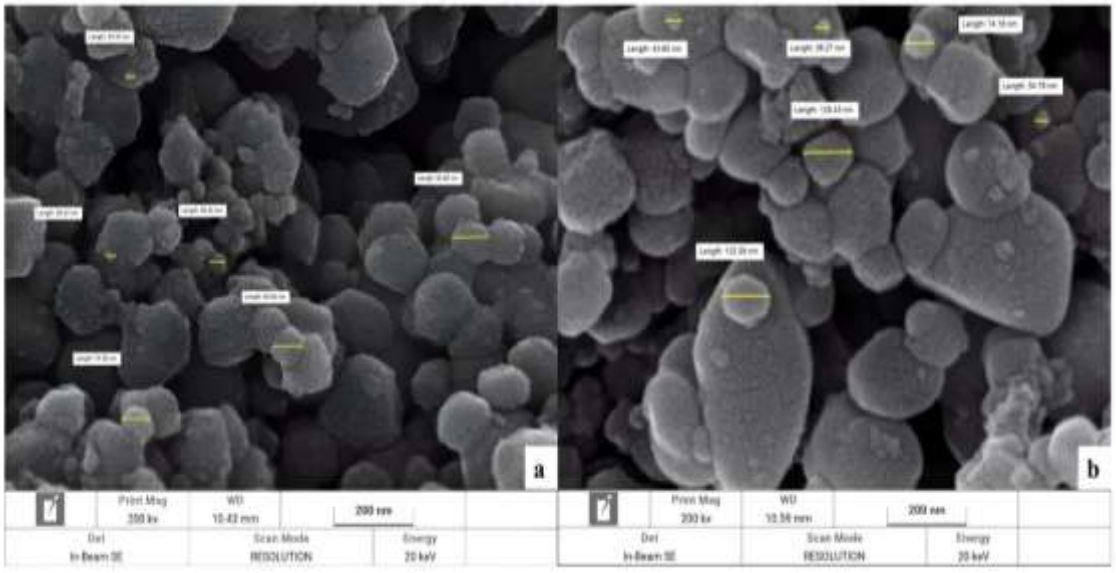

distribution and more pronounced agglomeration. The average particle size **(66 ± 4 nm)** reflects a less controlled growth process compared to the green synthesis route. The larger size and wider distribution may decrease surface reactivity and light absorption efficiency, which can influence photocatalytic activity.

Fig 4: FE-SEM and EDS of (a,c) green synthesis and (b,d) Chemical synthesis of N-TiO_2 NPs

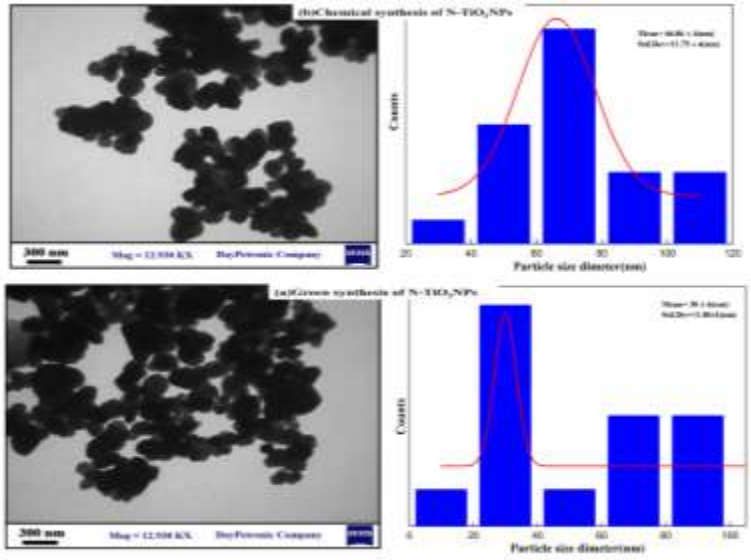

Fig 5: TEM of (a) green synthesis and (b) Chemical synthesis of N-TiO_2

FT-IR analysis

FTIR spectra of chemically and green-synthesized N-TiO_2 exhibit significant variations in surface functional groups, as shown in **Fig *6***. Chemically synthesized samples show well-defined peaks at 1620 cm^{-1} and 1384 cm^{-1} for water bending vibrations and nitrate or nitro groups. The existence of –OH groups by surface hydroxylation is reflected through a broad absorption between 3300 and 3500 cm^{-1}. In the green-synthesized sample, the peaks are broader and weaker, specifically at 1620 and 1400 cm^{-1}, because of organic molecules in the plant extract. There are bands in both spectra below 800 cm^{-1}, confirming the Ti–O–Ti bond and effective formation of TiO_2. Overall, the green process is seen to produce more functionalized and potentially less crystalline material than the chemical method, which gives a more organized one. These differences illustrate how the synthesis process affects the chemical structure and properties of N-TiO_2 [30].

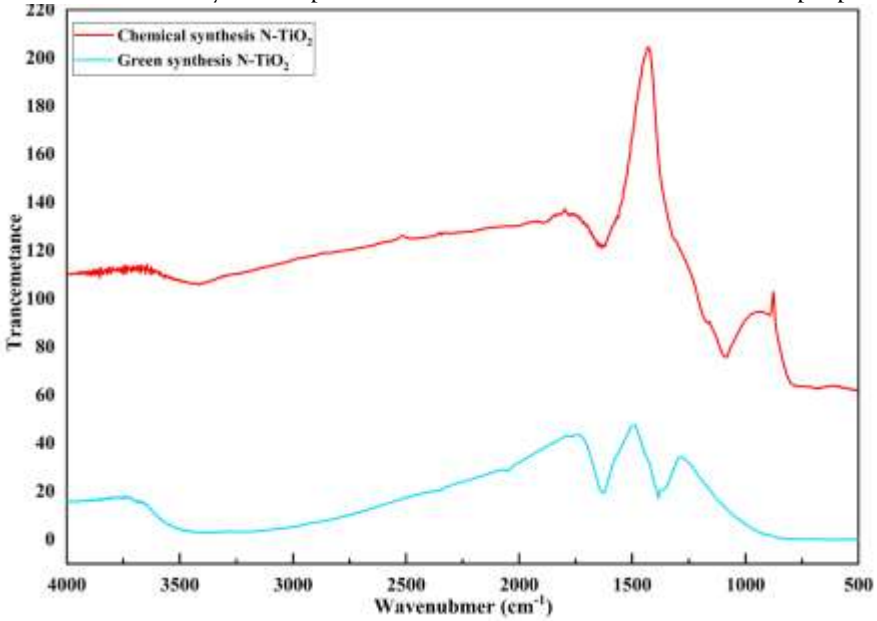

Fig 6: FT-IR spectra for green and chemical synthesis of N-TiO_2

UV-Vis-DRS analysis

As seen in **Fig 7**, ultraviolet-visible reflectance spectroscopy spectra indicate the extreme difference in optical behavior of chemically and green route prepared N-TiO2. The chemically prepared material exhibits a band gap of approximately 3.0 eV with absorption predominantly within the UV region. The N-TiO2 green synthesized, nonetheless, exhibits a smaller band gap of approximately 2.8 eV with red shift and higher visible range absorption. Nitrogen doping and the plant extract organic groups cause this diminution of the band gap. They may form intermediate energy states within the band structure. The increase in the visible light activity of the green-synthesized sample shows improved photocatalytic activity. The findings in **Fig 7** are confirmations that the synthesis process has an important impact on the optical and electronic properties of N-TiO_2. A Tauc plot study of $(\alpha hv)^{1/2}$ indirect transition against photon energy shows a noticeable decrease in the optical band gap, which confirms this discrepancy even further. The sample made with chemicals has a band gap of 2.95 eV, whereas the sample made with green chemicals has a band gap of 2.80 eV. These data confirm that the green sample responds better to visible light[31].

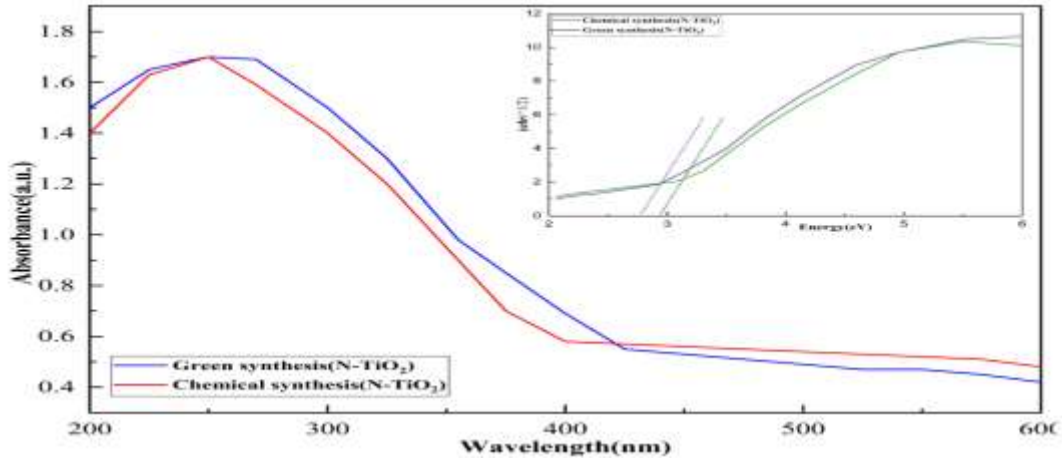

Fig 7: UV-Vis-spectroscopy for green and chemical N-TiO_2

Photocatalytic Activity

The photocatalytic activity of N-TiO_2 nanoparticles produced from green and chemical synthesis pathways was compared by observing the degradation of methyl orange (MO) under visible light irradiation at 464 nm. As evident in **Fig 8**, the green-synthesized N-TiO_2 showed much greater photocatalytic efficiency, degrading 86.6% of MO following the irradiation time. For comparison, the chemically synthesized N-TiO_2 showed a degradation efficiency of 73.3%, whereas the control experiment (catalyst without light irradiation) yielded only 3.9% degradation, affirming the critical role of the photocatalyst in the reaction. The higher activity of the green-synthesized sample can be due to the synergetic effect of nitrogen doping and the bio-mediated process of synthesis that likely introduced surface functional groups and oxygen vacancies. Such characteristics can lead to improved adsorption of dye molecules and facilitate the separation and transportation of photogenerated electron–hole pairs. Nitrogen doping, in addition, effectively reduces the band gap of TiO_2, enabling higher absorption in the visible range and improving the photocatalyst's response to irradiation. Collectively, these findings confirm that the method of green synthesis is not only an environmentally friendly alternative but also improves the photocatalytic degradation efficiency of N-TiO_2 under visible light irradiation.

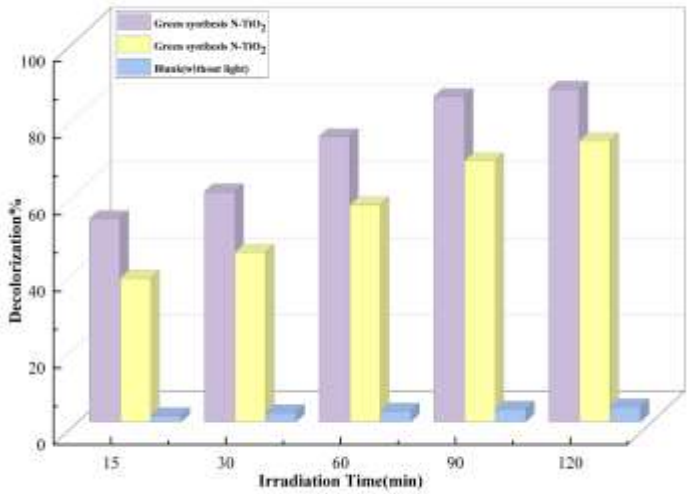

Fig 8: Photocatalytic activity of N-TiO_2 under visible light irradiation

Comparative Analysis of N-TiO_2 Synthesis Techniques for Photocatalytic Dye Degradation

The photocatalytic performance of N-TiO_2 is significantly influenced by the method of synthesis, nitrogen precursor, and operational conditions. Conventional sol–gel, solvothermal, thermal decomposition, and direct calcination routes have exhibited varied degradation efficiency against a series of dye pollutants. The sol–gel route, while offering good control over particle morphology, demonstrated comparatively low degradation activity under visible light with typically prolonged reaction duration. In contrast, the solvothermal route exhibited enhanced photocatalytic activity with appreciable degradation of dyes, but at the cost of extended treatment duration. Direct calcination of titanium nitride produced improved degradation efficiency in a reduced timeframe, demonstrating the benefit of nitrogen-rich precursors. Notably, the current study demonstrates the effectiveness of green-synthesized N-TiO_2, which exhibited 86.8% degradation of methyl orange within 120 minutes under light, outperforming the chemically synthesized N-TiO2 (73.3%) under identical conditions. Such comparative results demonstrated in **Table 1**, unequivocally demonstrate the potential of the green synthesis route as a green and highly effective method for the synthesis of visible-light-active photocatalysts for environmental remediation.

Table 1: Comparison of synthesis method N-TiO_2 and its use in the degradation of dye

No.	Synthesis method	Percussor of Nitrogen doping	Dye model	Optimal condition	Degradation%	Reference
1.	Thermal decomposition	annular grade TiO_2	Indigo carmine dye	DRS.pdf		[31]
2.	Sol–gel method	Titanium-n-butoxide	Bisphenol A (BPA) and Black 5 (RB5) Dye	360 min Under light	BAP=11.3% RB5=9.1%	[32]
3.	Sol–gel method	Titanium tetraisopropoxide	Blue5	75 min Under light	30%	[33]
4.	Solvothermal	Titanium (IV) butoxide	Methylene blue	500 min Under light	90%	[23]
5.	Direct calcining TiN	Titanium nitride (TiN)	4-chlorophenol (4-CP) and	240 min Under light	87.7%	[28]

			methylene blue (MB)			
6.	Current work Green synthesis N-TiO_2 Chemical synthesis N-TiO_2	Titanium tetraisopropoxide	Methyl orange	120 min Under light	86.8% 73.3%	-

Future Recommendations

– **Optimization of Parameters for Green Synthesis**

Additional research should investigate the influence of parameters like pH, calcination temperature, dopant concentration, and plant extract type on the structural and photocatalytic activity of N-TiO_2.

– **Exploration of Bio-Templates**

Exploring a broader variety of green sources—like various plant extracts or agricultural residue—can impart useful functional groups and improve absorption of visible light.

– **Formation of Heterostructures**

Future studies are suggested to explore the coupling of N-doped TiO_2 with other semiconductors (e.g., g-C_3N_4, ZnO) or carbon materials to enhance charge separation and extend the light absorption spectrum.

– **Real-World Application Studies**

Stability, reusability, and activity of the photocatalyst must be evaluated in sunlight and in actual wastewater samples to verify practical usability. Environmental and Economic Assessment. Life cycle assessment and cost analysis are suggested to guarantee the sustainability and scalability of the green synthesis method.

CONCLUSION

The present work presents a comparative assessment of nitrogen-doped TiO_2 nanoparticles prepared through green and chemical routes for their structural, optical, and photocatalytic properties. Bio-mediated synthesis involving the use of Taraxacum officinale extract resulted in nanoparticles with higher crystallinity, lower particle sizes, and greater nitrogen doping efficiency. These structural benefits were reflected in their higher photocatalytic activity, with 86.6% degradation of MO under visible light, in comparison with 73.3% from chemically synthesized counterparts. The lowered band gap energy and enhanced charge carrier dynamics in the green-synthesized N–TiO_2 are reasoned to be due to the synergetic impacts of nitrogen doping and bio-active molecules present in the plant extract. The work not only corroborates green synthesis as an efficient and environmentally friendly alternative to conventional chemical processes but also highlights its prospects for practical environmental remediation applications. Future efforts should be directed toward optimizing the synthesis parameters, extension to other bio-resources, and integrating N–TiO_2 with co-catalysts or heterojunction systems to further augment light absorption and charge separation efficiency

Acknowledgment: The authors appreciate Salahaddin University-Erbil and the University of Garmian for supporting this research.

Funding: No external funding was utilized

Data Availability: Data for the findings of this study are available on reasonable request from the corresponding author.

Decleration

The authors declare no conflicts of interest.

REFERENCE

[1] I. Journal *et al.*, "a Review of Nanoparticles: Their Synthesis, Properties, Application, and Advantages," *MINAR Int. J. Appl. Sci. Technol.*, vol. 06, no. 03, 2024, doi: 10.47832/2717-8234.20.4.

[2] N. Al-Harbi and N. K. Abd-Elrahman, "Physical methods for preparation of nanomaterials, their characterization and applications: a review," *J. Umm Al-Qura Univ. Appl. Sci.*, vol. 11, no. 2, pp. 356–377, 2025, doi: 10.1007/s43994-024-00165-7.

[3] D. Nunes *et al.*, "Metal oxide nanostructures for sensor applications," *Semicond. Sci. Technol.*, vol. 34, Mar. 2019, doi: 10.1088/1361-6641/ab011e.

[4] S. K. -, D. V. Y. -, and D. A. N. -, "A Study of Characteristics and Properties of Nano-metal Oxides (Zinc Oxide, Cadmium Oxide, Titanium Dioxide, Iron Oxide)," *Int. J. Multidiscip. Res.*, vol. 6, no. 4, pp. 1–19, 2024, doi: 10.36948/ijfmr.2024.v06i04.24617.

[5] V. Verma, M. Al-Dossari, J. Singh, M. Rawat, M. G. M. Kordy, and M. Shaban, "A Review on Green Synthesis of TiO2 NPs: Synthesis and Applications in Photocatalysis and Antimicrobial," *Polymers (Basel).*, vol. 14, no. 7, 2022, doi: 10.3390/polym14071444.

[6] J. M. Rzaij and A. M. Abass, "Review on: TiO2 Thin Film as a Metal Oxide Gas Sensor," *J. Chem. Rev.*, vol. 2, no. 2, pp. 114–121, 2020, doi: 10.33945/SAMI/JCR.2020.2.4.

[7] C. Song *et al.*, "TiO2-Based Catalysts with Various Structures for Photocatalytic Application: A Review," *Catalysts*, vol. 14, no. 6, 2024, doi: 10.3390/catal14060366.

[8] P. C. Dathan *et al.*, "A Review on Biomedical Applications of Titanium Dioxide," *Trends Biomater. Artif. Organs*, vol. 37, no. 1, pp. 49–54, 2023.

[9] J. Esmaeilzadeh, B. Raissi, A. K. Zak, and A. M. Hashim, "Fabrication of NO2 High-Temperature TiO2 Nanorods Gas Sensor and Study of Their Morphology and Arrangement Effects on the Sensing Behaviors," *Russ. J. Inorg. Chem.*, vol. 68, no. 14, pp. 1993–2000, 2023, doi: 10.1134/S0036023623602635.

[10] A. Kunka Ravindran, S. Narendhiran, B. Nambiraj, G. L. Muthusamy Anandan, S. P. Muthu, and R. Perumalsamy, "Catalyzing the Affordability of Perovskite Solar Cells with Aluminum-Modified Cubic Titania," *ACS Appl. Opt. Mater.*, vol. 2, no. 1, pp. 230–243, 2024, doi: 10.1021/acsaom.3c00410.

[11] X. Yang, R. Zhao, H. Zhan, H. Zhao, Y. Duan, and Z. Shen, "Modified Titanium dioxide-based photocatalysts for water treatment: Mini review," *Environ. Funct. Mater.*, vol. 3, no. 1, pp. 1–12, 2024, doi: 10.1016/j.efmat.2024.07.002.

[12] L. Ma, I. Jia, X. Guo, and L. Xiang, "High performance of Pd catalysts on bimodal mesopore for the silica catalytic oxidation of toluene," *Chinese J. Catal.*, vol. 35, no. 0, pp. 108–119, 2014, doi: 10.1016/S1872.

[13] R. Rashid *et al.*, "Advancements in TiO2-based photocatalysis for environmental remediation: Strategies for enhancing visible-light-driven activity," *Chemosphere*, vol. 349, p. 140703, 2024, doi: https://doi.org/10.1016/j.chemosphere.2023.140703.

[14] A. K. John and S. Palaty, "Green synthesis of nitrogen-doped TiO2 nanoparticles with exposed {001} facets using Chromolaena odorata leaf extract for photodegradation of pollutants under visible light," *Nano-Structures & Nano-Objects*, vol. 40, p. 101402, 2024, doi: https://doi.org/10.1016/j.nanoso.2024.101402.

[15] A. M. Elbasiony, A. A. Alamri, U. A. Soliman, H. G. Mohamedbakr, A. M. Wahba, and E. T. Helmy, "Green synthesis of N, B co-doped TiO2 nanoparticles with enhanced photocatalytic and antioxidant activities," *J. Taiwan Inst. Chem. Eng.*, p. 105626, 2024, doi: https://doi.org/10.1016/j.jtice.2024.105626.

[16] O. Sacco, A. Mancuso, V. Venditto, S. Pragliola, and V. Vaiano, "Behavior of N-Doped TiO2 and N-Doped ZnO in Photocatalytic Azo Dye Degradation under UV and Visible Light Irradiation: A Preliminary Investigation," *Catalysts*, vol. 12, no. 10, 2022, doi: 10.3390/catal12101208.

[17] C. Sanchez Tobon, D. Ljubas, V. Mandić, I. Panžić, G. Matijašić, and L. Ćurković, "Microwave-Assisted Synthesis of N/TiO(2) Nanoparticles for Photocatalysis under Different Irradiation Spectra.," *Nanomater. (Basel, Switzerland)*, vol. 12, no. 9, Apr. 2022, doi: 10.3390/nano12091473.

[18] N. Bao, J.-J. Niu, Y. Li, G.-L. Wu, and X.-H. Yu, "Low-temperature hydrothermal synthesis of N-doped TiO2 from small-molecule amine systems and their photocatalytic activity.," *Environ. Technol.*, vol. 34, no. 21–24, pp. 2939–2949, 2013, doi: 10.1080/09593330.2012.725772.

[19] T. H. Kim, G.-M. Go, H.-B. Cho, Y. Song, C.-G. Lee, and Y.-H. Choa, "A Novel Synthetic Method for N Doped TiO(2) Nanoparticles Through Plasma-Assisted Electrolysis and Photocatalytic Activity in the Visible Region.," *Front. Chem.*, vol. 6, p. 458, 2018, doi: 10.3389/fchem.2018.00458.

[20] D. V. Wellia, M. R. Habibillah, A. Syafawi, R. Rahmadini, R. Rahmayeni, and N. Pratiwi, "A New Combination Method of N-doped TiO2 Nanoparticles Synthesis for Heavy Metal Ions Cr(VI) Photoreduction Applications," *J. Kim. Sains dan Apl. Vol 26, No 2 Vol. 26 Issue 2 Year 2023DO - 10.14710/jksa.26.2.70-78* , Mar. 2023, [Online]. Available: https://ejournal.undip.ac.id/index.php/ksa/article/view/51395

[21] S. R. Miditana, S. R. Tirukkovalluri, I. M. Raju, A. B. Babu, and A. R. Babu, "Review on the synthesis of doped TiO2 nanomaterials by Sol-gel method and description of experimental techniques," *J. Water Environ. Nanotechnol.*, vol. 7, no. 2, pp. 218–229, 2022, doi: 10.22090/jwent.2022.02.008.

[22] H. RASOULNEZHAD, G. HOSSEINZADEH, R. HOSSEINZADEH, and N. GHASEMIAN, "Preparation of transparent nanostructured N-doped TiO2 thin films by combination of sonochemical and CVD methods with visible light photocatalytic

activity," *J. Adv. Ceram.*, vol. 7, no. 3, pp. 185–196, 2018, doi: 10.1007/s40145-018-0270-8.
[23] S. Samangsri, S. Chiarakorn, and T. Areerob, "Synthesis of N-doped TiO2 Nanoparticle by Solvothermal Method for Dye Treatment," *IOP Conf. Ser. Mater. Sci. Eng.*, vol. 576, no. 1, 2019, doi: 10.1088/1757-899X/576/1/012033.
[24] M. Yalcin, "The effect of pH on the physical and structural properties of TiO2 nanoparticles," *J. Cryst. Growth*, vol. 585, p. 126603, 2022, doi: https://doi.org/10.1016/j.jcrysgro.2022.126603.
[25] S. Manchwari, J. Khatter, and R. P. Chauhan, "Modifications in structural, morphological and optical properties of TiO2 nanoparticles: effect of pH," *Chem. Pap.*, vol. 76, no. 12, pp. 7545–7551, 2022, doi: 10.1007/s11696-022-02437-0.
[26] C. Y. Hsu *et al.*, "Nano titanium oxide (nano-TiO2): A review of synthesis methods, properties, and applications," *Case Stud. Chem. Environ. Eng.*, vol. 9, no. January, p. 100626, 2024, doi: 10.1016/j.cscee.2024.100626.
[27] M. E. Kassalia, Z. Nikolaou, and E. A. Pavlatou, "Photocatalytic Testing Protocol for N-Doped TiO2 Nanostructured Particles under Visible Light Irradiation Using the Statistical Taguchi Experimental Design," *Appl. Sci.*, vol. 13, no. 2, 2023, doi: 10.3390/app13020774.
[28] J. Liu, X. Li, H. Hou, and M. Zhou, "Facile synthesis of anatase–rutile diphase n-doped tio2 nanoparticles with excellent visible light photocatalytic activity," *Catalysts*, vol. 10, no. 10, pp. 1–13, 2020, doi: 10.3390/catal10101126.
[29] H. Li *et al.*, "Synthesis and characterization of N-doped porous TiO2 hollow spheres and their photocatalytic and optical properties," *Materials (Basel).*, vol. 9, no. 10, 2016, doi: 10.3390/ma9100849.
[30] P. V. Bakre, S. G. Tilve, and R. N. Shirsat, "Influence of N sources on the photocatalytic activity of N-doped TiO2," *Arab. J. Chem.*, vol. 13, no. 11, pp. 7637–7651, 2020, doi: 10.1016/j.arabjc.2020.09.001.
[31] "Synthesis of Nitrogen Doped Titanium Dioxide (TiO2) and its Photocatalytic Performance for the Degradation of Indigo Carmine Dye," *J. Environ. Nanotechnol.*, vol. 2, no. 1, pp. 28–31, 2013, doi: 10.13074/jent.2013.02.121026.
[32] R. Kamaludin, M. H. D. Othman, S. H. S. A. Kadir, A. F. Ismail, M. A. Rahman, and J. Jaafar, "Visible-Light-Driven Photocatalytic N-Doped TiO2 for Degradation of Bisphenol A (BPA) and Reactive Black 5 (RB5) Dye," *Water. Air. Soil Pollut.*, vol. 229, no. 11, 2018, doi: 10.1007/s11270-018-4006-8.
[33] J. T. Mehrabad, M. Partovi, F. A. Rad, and R. Khalilnezhad, "Ournal of," vol. 9, no. 3, pp. 233–239, 2019.